Published in final edited form as:
Nat Immunol. 2007 July ; 8(7): 732–742.

Comprehensive epigenetic profiling identifies multiple distal regulatory elements directing *Ifng* transcription

Jamie R. Schoenborn[1,2], **Michael Dorschner**[3,5,7], **Masayuki Sekimata**[1,7], **Deanna Santer**[1], **Maria Shnyreva**[1], **David R. Fitzpatrick**[4,6], **John A. Stamatoyannopoulos**[3,5], and **Christopher B. Wilson**[1]

1 *Department of Immunology, University of Washington, Seattle, Washington 98195*

3 *Department of Medicine, University of Washington, Seattle, Washington 98195*

5 *Department of Genome Sciences, University of Washington, Seattle, Washington 98195*

2 *Department of Graduate Program in Molecular and Cellular Biology, University of Washington, Seattle, Washington 98195*

4 *Amgen, Inc, Seattle, Washington 98119*

6 *PO Box 270514, Fort Collins, Colorado 80527-0514*

Abstract

Unlike the well-defined T_H2 cytokine locus, little is known regarding regulatory elements that govern expression of *Ifng*, which encodes the signature T_H1 cytokine interferon-γ. Evolutionary analysis revealed that the murine *Ifng* locus diverges from the ancestral locus due to structural rearrangements that delete the neighboring *Il26* gene and disrupt synteny 57 kb upstream of *Ifng*. Proximal to this disruption, we identified by high-resolution mapping multiple regions with $CD4^+$ T cell subset-specific epigenetic modifications. A subset of these regions were enhancers, while some blocked the activity of upstream enhancers or insulated *Ifng* from neighboring chromatin. These findings suggest that proper expression of *Ifng* is maintained through the collective action of multiple distal regulatory elements present in a ~100 kb region flanking *Ifng*.

Interferon-γ (IFN-γ) is produced in response to viral or intracellular bacterial infection and functions to activate macrophages, increase major histocompatibility complex (MHC) molecule expression and exert direct antiviral activity on infected cells. While natural killer (NK) and $CD8^+$ T cells are programmed to rapidly produce IFN-γ upon activation, $CD4^+$ T cells can adopt varied programs of effector function. The T helper 1 (T_H1) and T_H2 lineages are the most well characterized CD4 programs: T_H1 effectors produce large amounts of IFN-γ, while T_H2 effectors produce little IFN-γ but large amounts of interleukin 4 (IL-4), IL-13 and IL-5. Proper cytokine expression and commitment to these lineages is primarily regulated at the level of transcription, with the transcription factors T-bet and GATA-3 dictating the commitment to T_H1 and T_H2 lineages, respectively[1–4]. T-bet directs this commitment by repressing GATA-3[5,6], remodeling the *Ifng* locus, aiding in transcription of *Ifng*[7], and inducing expression of IL-12Rβ2[8] and the transcription factor Hlx[9].

[7]These authors contributed equally.

Author contributions

J.R.S. designed and performed research, analyzed data and wrote the paper; M.O.D. designed and performed research and analyzed data; M.Se. performed research and analyzed data; D.M. S. performed research and analyzed data; M.Sh. performed the ChIP on D10 and AE7 cells; D.R.F. contributed intellectually and helped write the paper; J.A.S. designed research; C.B.W. designed research, analyzed data and wrote the paper; all authors reviewed the paper before submission.

The signaling events and transcription factors that drive IFN-γ expression have been elucidated in considerable detail, but relatively little is known regarding where and how they act[2,10]. Transgenes containing the *Ifng* promoter, introns and up to 3.4 kb of 5′ flanking sequence do not confer proper T cell subset-specific expression *in vivo*[11–13]. By contrast, a 191 kb bacterial artificial chromosome transgene containing the human *IFNG* gene and 90–95 kb of flanking sequence results in high-level, T_H1-specific IFN-γ production[13]. This result suggests that distal transcriptional regulatory elements are required for proper expression, the necessary elements are present within this extended region, and that elements from the human *IFNG* locus are sufficiently conserved to function properly in mice.

Distal regulatory elements aid in chromatin remodeling to establish and maintain lineage-specific programs of gene expression and are often highly conserved among species. Enhancers are necessary for high-level gene transcription, whereas silencers inhibit gene expression and may serve as foci that initiate permanent silencing in non-expressing cell types. The separation of genomic DNA into domains with distinct gene expression patterns is thought to be mediated, at least in part, by boundary elements[14,15]. Boundary elements include insulators, which act as barriers to restrict the spread of repressive heterochromatin, and enhancer-blocking elements that shield genes from the long-range effects of enhancers or silencers associated with adjacent genes[10,16]. Regulatory elements are usually located within 50–75 kb of the gene they regulate, but can be located up to several hundred kilobases away, and are commonly found in open chromatin, where transcription factors and other protein mediators are able to access specific DNA sequences to control gene expression. Thus, in addition to sequence conservation[17], focal changes in chromatin structure and DNA methylation have been used to predict the location of distal regulatory elements within gene loci[10,18].

In this study, we have used computational, chromatin-based and functional approaches to identify distal regulatory elements that help to govern *Ifng* expression in $CD4^+$ T cells. Comparative genomic analysis revealed eight highly conserved non-coding sequences (CNSs) surrounding *Ifng*. Using an innovative, PCR-based method to map DNase hypersensitive (HS) sites in a comprehensive and sequence-specific manner[18], along with chromatin immunoprecipitation (ChIP) and DNA methylation analysis, we demonstrate distinct $CD4^+$ T cell subset-specific epigenetic marks at and around these CNSs. A subset of these sequences enhanced IFN-γ expression in response to signals downstream of the TCR, cytokine receptors, and/or T-bet, while some acted as insulators or enhancer-blocking elements, suggesting that proper expression of *Ifng* is governed in part by the collaboration of multiple regulatory elements in an ~100 kb region surrounding *Ifng*.

RESULTS

Conservation and divergence in the *Ifng* locus

To identify regulatory elements in the *Ifng* locus, we first performed a multi-species alignment using the mouse genome as base. Syntenic regions of mouse chromosome 10, rat chromosome 7 and human chromosome 12 are shown in Fig. 1. In each of these species, the *Il22* and *Mdm1* genes are located upstream of *Ifng*. *Mdm1* is a highly conserved p53-binding protein and *Il22* encodes a pro-inflammatory member of the IL-10 cytokine family. The *IL26* gene, which like *IL22* is a member of the IL-10 cytokine family, is located between *IL22* and *IFNG* in humans, bony fish[19] and all available mammalian genomes except rodents. In rodents, *Il26* has been disrupted by a LINE insertion and an LTR-LINE-LTR insertion located 57–59 and 73–87 kb upstream of murine *Ifng*, respectively (Fig. 1a, Supplementary Fig. 1 online). C57BL/6 and 129/Sv mice also contain *Iltifβ*[20], which represents an inverted duplication of the *Il22* gene and is flanked on either side by six tandem repeats containing a highly conserved 1 kb core with homology to mouse chromosome 12 and human chromosome 6 (http://eichlerlab.gs.washington.edu/database.html). Downstream of *Ifng* there are no known coding

genes for ~420 kb, but a non-coding antisense transcript[21], *Tmevpg1*, begins 120 kb downstream of *Ifng* and extends to within 61 kb of the *Ifng* start site.

Despite the striking structural differences in the *Ifng* locus between rodents and humans, patterns of *Ifng* expression in specific cell types are substantially similar in these species. This similarity indicates that regulatory elements involved in *Ifng* expression are not affected by these structural differences and suggests that most, if not all, such regulatory elements are likely to be not more than 57 kb upstream of *Ifng*. For this reason, we searched for CNSs in this region and for a similar distance downstream of *Ifng*. We identified eight CNSs, which are denoted by the distance of their 5′ end relative to the start of murine *Ifng*, and include the previously identified CNS1 and CNS2 (refs. 22,[23]), referred to herein as *Ifng*CNS-6 and *Ifng*CNS+18–20, respectively (Fig. 1c). None of these CNSs correspond to known open reading frames, suggesting that they may contain regulatory elements.

While sequence conservation is one approach by which to identify candidate regulatory elements, the correlation between conservation and function is imperfect[10,17,24]. Regulatory elements can also be identified experimentally through the detection of epigenetic modifications that are typical for such regions. To provide a substrate by which to determine the epigenetic profile of the *Ifng* locus in $CD4^+$ T cell subsets, we isolated naive $CD4^+$ T cells from Smarta TCR-transgenic mice and studied these cells directly *ex vivo* or after differentiation *in vitro* in T_H1 or T_H2 conditions for eight days (Supplementary Fig. 2 online).

Localization of DNase HS sites in the *Ifng* locus

Regulatory elements are commonly distinguished by a marked sensitivity to cleavage by DNase I and have traditionally been identified using the Southern transfer and indirect end-labeling approach. This technique depends on suitable positioning of restriction sites, availability of flanking probes, and does not precisely localize the hypersensitive sequences. To overcome these limitations, we employed a sequence-specific PCR-based approach, which is quantitative and localizes HS sites with a resolution of ~225–250 base pairs[18]. We used this approach to search for regulatory elements in an unbiased manner over 114 kb extending upstream of *Ifng* to the region where synteny is disrupted and downstream to the terminus of the *Tmevpg1* antisense transcript. The results are displayed in Fig. 2, in which peaks denote HS sites and peak height the degree of hypersensitivity.

Within this region, we confirmed the presence of HS sites I, II and III, located at the *Ifng* promoter, intron 1 and intron 3, respectively, which were previously defined in the long-term D5 T_H1 cell line[25]. There has been some ambiguity as to whether HSI is in the promoter or proximal first intron[22,25]. Our studies showed HSI to be at the promoter in primary T_H1 cells (Fig. 2). These 3 HS sites, particularly HSII, were weak compared to the strong HS+18 site, which coincides with the 5′ end of IfngCNS+18–20, as previously demonstrated by Southern blot[23]. An HS site coinciding with *Ifng*CNS-6, demonstrated to date only in restimulated D5 cells[22], was not consistently evident in primary T_H1 cells.

In addition to HS+18, we detected several strong HS sites (strong HS sites are denoted as HS and weak sites as hs followed by distance in kb from the *Ifng* start) not identified previously. HS-22, which lies within *Ifng*CNS-22, was detected in T_H1 and T_H2 cells but not in naive $CD4^+$ T cells, a pattern similar to that of HSIII. By contrast, HS+29, which coincided with *Ifng*CNS+29, was T_H1-specific, like HS+18, HSI and HSII. Somewhat surprisingly, four strong sites, HS−40, HS−35, HS+8 and HS+26 were T_H2-specific, a fifth, HS+49, was strong in T_H2, intermediate in naive $CD4^+$ T cells but just above background in T_H1 cells, and a sixth, hs+53 was intermediate in naïve, weak in T_H1 and absent in T_H2 $CD4^+$ T cells. By contrast to the strong HS sites detected in T_H1 cells, each of which was located within a CNS, the five HS sites restricted to or strongest in T_H2 or naive $CD4^+$ T cells were adjacent to but not within a

CNS (Fig. 2 and Supplementary Table 1 online). The location of these sites adjacent to CNSs may reflect nucleosome sliding or displacement from nearby or clustered regulatory elements that are employed differentially in T_H1 cells versus T_H2 and naïve $CD4^+$ T cells. This pattern also held true for weak hs sites (Fig. 2) with but two exceptions: the weak T_H1-specific hs+36 did not coincide with a CNS, and the T_H2-specific hs+55 coincided with *Ifng*CNS+55. These results demonstrate that the set of HS sites in T_H1 cells is distinct from that in T_H2 and naive $CD4^+$ T cells, and suggest that there are multiple distal regulatory elements in the *Ifng* locus, which are likely to function in a $CD4^+$ T cell subset-specific manner.

Histone modifications in the *Ifng* locus

DNase HS sites are typically associated with transcriptionally permissive histone modifications. To test this prediction and to provide a complementary approach to search for regulatory elements in the *Ifng* locus, we scanned the locus by ChIP to detect histone H3 dimethyl lysine 4 (K4(me2)), a stable mark associated with poised or actively transcribed chromatin[24,26], and trimethyl lysine 27 (K27(me3)), a repressive histone modification associated with the establishment of Polycomb-mediated silencing[27,28]. DNase HS sites form where the nucleosomal array is distorted or displaced, potentially reducing total H3 abundance[29,30], whereas Polycomb-mediated silencing results in the compaction of nucleosomes thereby potentially increasing total H3 density[31]. To control for these possibilities, we also performed ChIP for total H3 and present results for K4(me2) and K27 (me3) both in absolute terms and relative to the abundance of H3 at that position (denoted K4 (me2)/H3 and K27(me3)/H3).

Naive $CD4^+$ T cells had little constitutive enrichment for K4(me2) throughout the *Ifng* locus, with the exception of low amounts found at *Ifng*CNS-34 and *Ifng*CNS-22 (Fig. 3a, top). In contrast, T_H1 cells were characterized by distinct peaks of K4(me2) at all CNSs except *Ifng*CNS+55. A broad area of K4(me2) enrichment was centered around *Ifng*CNS+29 and *Ifng*CNS+46 in T_H1 cells, supporting previous reports that K4(me2) enrichment may be found at regulatory regions of active genes even where the underlying DNA sequence is not highly conserved[24]. Surprisingly, T_H2 cells had moderate K4(me2) enrichment at *Ifng*CNS-22, and slight enrichment at the *Ifng* gene, *Ifng*CNS+18, *Ifng*CNS+29, and just 5′ of *Ifng*CNS+46. When corrected for the total abundance of H3 (Supplementary Fig. 3 online), the regions of apparent K4(me2) enrichment were substantially diminished in T_H2 and naïve $CD4^+$ T cells (Fig. 3b, top), while correction for total H3 abundance in T_H1 cells further sharpened the K4 (me2) peaks, most notably at *Ifng*CNS+29 and *Ifng*CNS+46, resolving K4(me2) to the regions of highest conservation. This pattern of K4(me2) enrichment largely mirrored that of H3 acetylation in long-term polarized T_H1 and T_H2 cell lines (Supplementary Fig. 4 online).

In contrast to the K4(me2) patterns observed, K27(me3) was present in naive $CD4^+$ and T_H2 cells but not in T_H1 cells (Fig. 3a,b, bottom). Naive $CD4^+$ cells had moderate amounts of K27 (me3) and K27(me3)/H3 in the region between *Ifng*CNS+29 and *Ifng*CNS+46. When differentiated into T_H2 cells, K27(me3) and K27(me3)/H3 increased in this region and spread throughout the *Ifng* gene and into the region upstream of *Ifng*CNS-22. By contrast, differentiation into T_H1 cells resulted in a near complete loss of K27(me3) and K27(me3)/H3 throughout the locus. Thus, while K4(me2) is largely a T_H1-specific modification most strongly associated with CNSs, K27(me3) is broadly distributed throughout the locus in T_H2 cells and only modestly enriched at CNSs.

Because the cytokine environment and commitment to effector cell lineage may differ between *in vitro*-derived T_H1 cells and T_H1 effectors generated *in vivo*, we also performed K4(me2) ChIP using T_H1 effector $CD4^+$ Smarta TCR-transgenic cells generated in response to lymphocytic choriomeningitis virus (LCMV) infection *in vivo* (Supplementary Fig. 2). Since the numbers of *in vivo* effectors were limited, we focused on regions that were most informative

with *in vitro*-derived cells. T_H1 effectors generated *in vivo* showed peaks of K4(me2) at *Ifng* and at each of the CNSs from *Ifng*CNS-34 to *Ifng*CNS+29, but compared to *in vitro*-derived T_H1 cells had relatively greater K4(me2) enrichment at *Ifng*CNS-6, less enrichment at *Ifng*CNS+46 and no enrichment at *Ifng*CNS-54 (Fig. 3c). Hence, K4(me2) enrichment did not extend to the most distant CNSs in $CD4^+$ T_H1 cells generated in response to LCMV infection as it did in *in vitro* derived T_H1 cells.

Cell lineage-specific demethylation in the *Ifng* locus

Unmethylated DNA is commonly associated with poised or active chromatin. Therefore elements involved in *Ifng* regulation are expected either to be demethylated in naive $CD4^+$ T cells or to become demethylated during T_H1 differentiation. In naive $CD4^+$ T cells, the majority of CpGs at *Ifng*CNS-34, *Ifng*CNS-22, the *Ifng* promoter, *Ifng*CNS+29 and *Ifng*CNS+46 were demethylated (Fig. 4a). By contrast, with the exception of *Ifng*CNS+46, each of these regions was largely methylated in hepatocytes, a cell type that cannot express *Ifng*. Compared to naïve $CD4^+$ T cells, T_H1 cells demonstrated substantial demethylation at *Ifng*CNS-54, intron 1 and *Ifng*CNS+18–20. In contrast, T_H2 cells gained CpG methylation at the *Ifng* promoter. A reciprocal pattern was seen at the *Il4–Il13* locus, with demethylation at CNS1 and the *Il4* promoter in T_H2 cells (Fig. 4b), as previously reported[32,33].

Along with results presented in the previous sections, these data indicate that the precise pattern of HS sites, K4(me2) and K27(me3) enrichment, and CpG methylation differ between naive, T_H1 and T_H2 cells (Fig. 5). T_H1 differentiation induced CpG demethylation at *Ifng*CNS-6, intron 1, and *Ifng*CNS+18–20, along with striking K4(me2) enrichment at all *Ifng*CNSs except *Ifng*CNS+55. Although not all regions enriched in K4(me2) in T_H1 cells had a corresponding DNase HS site, HS sites in T_H1 cells were exclusively found at such regions. In contrast, T_H2 effectors gained CpG methylation at the *Ifng* promoter, and K27(me3) increased throughout much of the locus. Unlike T_H1-specific DNase HS sites, T_H2-specific DNase HS sites were adjacent to CNSs and corresponded to regions where enrichment for K27(me3) was most evident. CNS-22 was notable in lacking CpG methylation, the presence of K4(me2) in naïve, T_H1 and T_H2 cells, and DNase hypersensitivity in both T_H1 and T_H2 cells. Collectively these epigenetic distinctions suggest differential utilization and function of distal regulatory elements in naïve, T_H1 and T_H2 $CD4^+$ T cells.

Distal elements can enhance IFN-γ production

To determine if any of the elements identified by epigenetic analyses were able to enhance IFN-γexpression, we transfected EL-4 T cells with plasmids containing a 9 kb murine *Ifng* gene (−3.4 to +5.6 kb) or the *Ifng* gene downstream of one of the elements identified by epigenetic analysis. Cells were also transfected with an empty expression vector or one directing expression of T-bet, plus an *Actb* promoter-driven *Renilla* luciferase transfection control plasmid. Transfected cells were then stimulated with PMA plus ionomycn, and transgene-driven production of IFN-γ was determined by ELISA and normalized to *Renilla* luciferase activity.

As previously reported, EL-4 cells produced little or no endogenous IFN-γ[23], but did so when transfected with the *Ifng* gene (Fig. 6a,b). In response to PMA plus ionomycin, cells transfected with the *Ifng*CNS+29 construct produced two to three times as much IFN-γ as the *Ifng* gene alone, as did cells transfected with the construct containing *Ifng*CNS-6, which was previously shown to enhance IFN-γ production[23]. A similar two- to three-fold increase was observed with these constructs in the presence of T-bet. By contrast, constructs containing *Ifng*CNS-22 and *Ifng*CNS-34 enhanced IFN-γ production only in stimulated, T-bet-transfected cells.

To assay for enhancer activity in additional cell types and in response to alternative stimuli, we cloned each element upstream of the -624bp *Ifng* promoter driving a firefly luciferase reporter. These constructs and a thymidine kinase (TK) promoter-driven renilla luciferase control were nucleofected into primary murine T_H0, T_H1 and T_H2 $CD4^+$ T cells and $CD8^+$ T cells, which were then stimulated with anti-CD3 and anti-CD28, IL-12 plus IL-18 or both. Primary NK cells could not be nucleofected, so we used the human NK-92 cell line to study NK cell responses.

In NK-92 cells, expression from each of these constructs increased in response to stimulation with IL-12 plus IL-18 or PMA plus ionomycin and was greatest in response to the combination of these stimuli (Fig. 7a). *Ifng*CNS-34, *Ifng*CNS-22, *Ifng*CNS-6, *Ifng*CNS+46, and to a lesser extent *Ifng*CNS-54, enhanced expression under all conditions. The degree of enhancement by *Ifng*CNS+46 was similar in non-stimulated cells and in cells stimulated with IL-12 plus IL-18, PMA plus ionomycin or the combination, suggesting that this element is primarily responsive to transcription factors that are constitutively expressed and active in NK cells, such as Eomes or T-bet. By contrast, *Ifng*CNS-22 disproportionately enhanced the response to IL-12 plus IL-18 (mean ± SD fold enhancement over the *Ifng* promoter alone = 5.75 ± 0.73), while *Ifng*CNS-6 (11.97 ± 0.45) and *Ifng*CNS-34 (11.58 ± 0.44), and to a lesser degree *Ifng*CNS-54 (4.34 ± 0.17), principally enhanced expression in response to PMA plus ionomycin. When these stimuli were used together a composite of their independent effects was observed. The ability of these elements to enhance expression in NK-92 cells also demonstrates that the function of these elements is conserved among humans and mice.

When these constructs were transfected into primary T cell subsets that express IFN-γi expression increased in response to stimulation with IL-12 plus IL-18 or anti-CD3 plus anti-CD28 and was greatest in response to the combination of these stimuli. As in NK-92 cells, *Ifng*CNS-6 enhanced expression in anti-CD3 plus anti-CD28-stimulated $CD8^+$ T cells (6.74 ± 0.25) and in T_H0 and T_H1 $CD4^+$ T cells (6.27 ± 0.17; Fig. 7b,c and data not shown); *Ifng*CNS-34 did so as well but only in $CD8^+$ T cells. *Ifng*CNS-22 enhanced expression in response to IL-12 plus IL-18 in T_H0 and T_H1 cells (2.14 ± 0.15), but this effect was not consistently evident in $CD8^+$ T cells. By contrast to the results in these T cell subsets, expression of each of these constructs in T_H2 cells was low and did not change in response to stimulation (Fig. 7d).

Thus, expression of these constructs was appropriately restricted to IFN-γ-producing cell subsets, and *Ifng*CNS-6, *Ifng*CNS-34, and *Ifng*CNS-22 enhanced expression both in the EL-4 and NK-92 cell lines and in primary T cells. *Ifng*CNS-6 and *Ifng*CNS-34 primarily enhanced expression in response to signals emanating from the TCR or NK receptors, *Ifng*CNS-22 primarily enhanced expression in response to IL-12 plus IL-18, and *Ifng*CNS-22 and *Ifng*CNS-34 were T-bet-dependent enhancers. Although *Ifng*CNS+29 enhanced expression in EL-4 cells as effectively as *Ifng*CNS-6, this activity was not detected in other cell types, suggesting that its activity may be limited to specific contexts.

Boundary elements in the *Ifng* locus

The presence of differentially expressed genes and structural rearrangements upstream of *Ifng* and the antisense *Tmevpg1* transcript downstream of *Ifng*, suggests that one or more of distal elements might function as boundary elements. To address this question, we utilized a colony-forming assay that tests the ability of elements to repress or stimulate the expression of a selectable marker when stably integrated into chromatin. EL-4 T cells were transfected with a plasmid containing a bacterial neomycin-resistance gene (*neo*^{r}) placed under the control of the promoter and enhancer from the human *TCRαδ*locus and flanked on the 3′ end by the *Drosophila* scs' insulator element, which prevents influence of downstream enhancers or heterochromatin[34,35]. Expression of *neo*^{r} is measured by colony formation after selection of

G418-resistant colonies in soft-agar (Fig. 8). CNS elements were then cloned 5′ of the enhancer to assay for insulator function indicated by increased colony formation, or were placed between the enhancer and promoter to assay for ability to block upstream enhancers, resulting in fewer colonies.

EL-4 cells transfected with the construct containing the *c-myc* 1.6 kb MINE insulator[35] cloned upstream of the enhancer as a positive control produced 2.3-fold more colonies than the β-Neo control construct (Fig. 8a). *Ifng*CNS+46 increased colony formation 2-fold when placed upstream of the enhancer, indicating its ability to function as an insulator and suggesting that it may form a functional 3′ locus boundary. The alternative interpretation – that *Ifng*CNS+46 acted as an enhancer – is not consistent with its inability to increase colony formation when placed between the enhancer and promoter (Fig. 8b) nor its inability to enhance expression of luciferase reporters in EL-4 cells (Fig 6). When EL-4 cells were transfected with constructs containing the 1.6 kb MINE enhancer-blocking element between the TCRδenhancer and promoter as a positive control, G418-resistant colonies were reduced to numbers similar to constructs lacking the enhancer (Fig. 8b). *Ifng*CNS-54, *Ifng*CNS-34 and *Ifng*CNS-22 also exhibited enhancer-blocking activity, decreasing the number of colonies to 10 to 26% of control values when cloned between the enhancer and promoter. The alternative interpretation – that these elements are silencers – is not consistent with their failure to reduce colony formation when placed upstream of the enhancer (Fig. 8a) nor with their ability to enhance expression in transient transfection assays (Figs. 6 and 7). These results suggest that these three upstream elements may protect *Ifng* from the influence of flanking sequences or regulatory elements associated with upstream genes or *vice versa*.

DISCUSSION

This report provides the first comprehensive computational and epigenetic analysis of the *Ifng* locus, which in concert with functional studies was used to delineate and characterize distal elements that regulate *Ifng* expression. The murine *Ifng* locus diverges from that of other mammals as a result of complex structural rearrangements commencing 57 kb upstream of *Ifng*. Despite these substantial differences in locus architecture, *Ifng* is expressed similarly in humans and mice, suggesting that regulatory elements necessary for proper *Ifng* expression are proximal to this divergence. Within ~60 kb upstream or downstream of murine *Ifng*, we identified eight CNSs, which displayed distinct patterns of K4(me2) and K27(me3), CpG methylation and overlying or adjacent DNase HS sites that differed between naive, T_H1 and T_H2 $CD4^+$ T cells. Functional studies showed that the most distal CNSs (*Ifng* CNS-54 and *Ifng* CNS+46) acted primarily as boundary elements, whereas the more proximal CNSs (*Ifng* CNS-34, *Ifng* CNS-22, *Ifng* CNS-6, and, in some contexts, *Ifng* CNS+29) were enhancers, two of which (*Ifng* CNS-34 and *Ifng*CNS-22) could also function as boundary elements. The T cell-subset specific epigenetic marks associated with these regulatory elements suggested that they function to control *Ifng* expression in a manner appropriate for that subset. Consistent with this notion, constructs containing these elements and the *Ifng* promoter were active in primary T cell subsets that express *Ifng* and repressed in T_H2 cells, which do not.

Naive $CD4^+$ T cells are poised to express low amounts of *Ifng* mRNA shortly after activation[36]. In these cells, the *Ifng* promoter lacks transcriptionally favorable histone marks and HS sites but has demethylated CpGs and is juxtaposed to the T_H2 cytokine locus, perhaps creating a hub that allows these two regions to compete for limiting transcription factors prior to fate specification[25,37–39]. We show here that the enhancers at *Ifng*CNS-34, *Ifng*CNS-22, and *Ifng*CNS+29 have demethylated CpGs in naive $CD4^+$ T cells, and that *Ifng*CNS-22 has modest amounts of the permissive K4(me2) histone modification, perhaps poising these elements to facilitate *Ifng* expression during the early stages of T_H1 differentiation. By contrast, CpGs in the two distal enhancers described previously, *Ifng*CNS-6 and *Ifng*CNS+18–20[22,

[23] and in the introns[13] are densely methylated in naive $CD4^+$ T cells, suggesting that these regions may amplify expression at later stages. *Ifng*CNS+46 was the other element with demethylated CpGs in naive $CD4^+$ T cells. This element appeared to act as an insulator in T cells, though it had some basal enhancer activity in NK cells. Naive $CD4^+$ T cells also contained two nearby HS sites (hs+49 and hs+53) and the surrounding region was modestly enriched for K27(me3). These two features were more prominent in T_H2 cells and markedly diminished in T_H1 cells, suggesting that the insulator activity of *Ifng*CNS+46 may serve to keep the locus poised in naive $CD4^+$ T cells by limiting the intrusion of repressive chromatin and/or encroachment by the downstream non-coding *Tmevpg1* transcript. This transcript is thought to negatively regulate *Ifng* based on expression of both *Ifng* and *Tmevpg1* by similar lymphocyte lineages, opposing expression patterns after stimulation, and the linkage of a genetic locus containing these regions with susceptibility to Theiler's encephalomyletis[21, 40]. The presence of K27(me3) has been suggested to serve as a mark for regulatory regions poised for silencing upon differentiation[41]. Thus, the region containing *Ifng*CNS+46, hs+49 and hs+53 may serve as a developmental switch region that protects *Ifng* locus accessibility in naive $CD4^+$ T cells, but facilitates silencing in T_H2 cells. In many respects, *Ifng*CNS+46 appears analogous to HSS3, which is located between the *Il4* and *Il13* genes. HSS3 is hypersensitive in naive, T_H1 and T_H2 cells, enriched in K27(me3) in naive and T_H1 cells and loses K27(me3) in T_H2 cells[42]. Though the function of HSS3 has not been tested, we speculate that it too may act as an insulator.

Compared to naive $CD4^+$ T cells, high-level T_H1-specific IFN-γ expression requires increased transcriptional accessibility at the *Ifng* locus. T_H1 differentiation is known to be associated with progressive CpG demethylation and acquisition of DNase HS at *Ifng*CNS-6, the *Ifng* promoter and intronic enhancers, and *Ifng*CNS+18–20[9,22,23,25]. We found that T_H1 cells also acquired strong HS sites at two additional enhancers, *Ifng*CNS-22 and *Ifng*CNS+29, weak hs sites hs+36 and hs+46, and peaks of K4(me2) corresponding to the *Ifng* promoter and gene and each of the enhancers identified here and in previous reports. T_H1 commitment also resulted in the complete loss of K27(me3) in the locus. *Ifng*CNS+46, *Ifng*CNS+29, *Ifng*CNS-22 and *Ifng*CNS-34 lacked CpG methylation in naïve CD4 T cells, suggesting that they may interact with the *Ifng* promoter in naive $CD4^+$ cells, as does the most proximal enhancer *Ifng*CNS-6[39]. Early signaling events following stimulation may target these elements to begin structural chromatin changes and three-dimensional rearrangement of the *Ifng* locus, resulting in the recruitment of other elements necessary for high-level, heritable IFN-γ production. While this manuscript was in preparation, another report also identified *Ifng*CNS-22 and *Ifng*CNS-34 and showed, as we have, that these act as T-bet dependent enhancers[43]. However, in contrast to our findings and to previous reports[22,23], they did not show enhancer function for *Ifng*CNS-6, which may reflect differences in reporter constructs. They also demonstrated that deletion of *Ifng*CNS-22 from a BAC Thy1.1-reporter transgene resulted in a marked loss of reporter expression by T_H1, $CD8^+$ T and NK cells, indicating that this element is also key *in vivo*. Together these data suggest that multiple distal enhancers located upstream and downstream of *Ifng* promote its expression in response to signals from the TCR and from the canonical T_H1 master regulator T-bet. Others have shown that histone acetylation in the *Ifng* locus of T_H1 cells is dependent on T-bet and STAT-4[44], however a more precise mapping will be needed to define the elements mediating these effects.

In addition to enhancers, proper expression of genes requires that they be protected by boundary elements from the unwanted effects of regulatory elements associated with nearby genes and surrounding chromatin domains. Four elements with boundary function were detected in the *Ifng* locus, each of which was marked by K4(me2) and demethylated CpGs in T_H1 cells. As noted above, *Ifng*CNS+46 may insulate the locus from encroachment by repressive K27(me3). Upstream, *Ifng*CNS-22, *Ifng*CNS-34, and *Ifng*CNS-54 may serve as sequential barriers helping to segregate *Ifng* from upstream transposable elements and segmental duplications and from

the regulatory elements associated with *Il22* and *Mdm1* or vice versa. Transposable and repetitive elements can alter the epigenetic structure of surrounding chromatin resulting in activation or silencing of nearby genes [45]. And while IL-22, like IFN-γ, is an effector cytokine expressed minimally or not at all by naive T cells[46], unlike IFN-γ, IL-22 is highly expressed by T_H-17 rather than T_H1 cells[47]. In addition to their boundary function, *Ifng*CNS-34 and *Ifng*CNS-22 were found to be T-bet-dependent enhancers, and *Ifng*CNS-22 enhanced expression in response to IL-12 plus IL-18, suggesting that these elements are capable of binding multiple proteins with distinct functions. The factors that mediate these distinct functions will need to be elucidated to completely understand how these elements are involved in *Ifng* expression.

In contrast to T_H1 cells, T_H2 cells must silence *Ifng* to prevent its erroneous expression[10, 33,42]. We show here that in T_H2 cells K27(me3) spreads, extending from *Ifng*CNS+46 to include the *Ifng* gene and upstream of *Ifng*CNS-22. This spreading is characteristic of Polycomb-mediated gene silencing[28], which has previously been described for the T_H2 cytokine locus in T_H1 cells[48]. The distribution of K27(me3) in T_H2 cells compared to naive $CD4^+$ T cells was suggestive of a bidirectional process, one extending from the region around *Ifng*CNS+29 and *Ifng*CNS+46 upstream to envelope the *Ifng* gene, and the other commencing upstream and extending down to *Ifng*CNS-22. In parallel, multiple T_H2-specific HS sites were acquired, and HS-35 and HS+49 became stronger than in naive $CD4^+$ T cells. The location of these HS sites relative to the spreading of K27(me3) raises the possibility that these sites may represent locations from which the spreading is orchestrated. Conversely, HS-22 is strong in both T_H1 and T_H2 cells and is located at the upstream boundary of K27(me3), suggesting that it may block further spreading of this repressive mark perhaps to maintain some measure of plasticity in cells proceeding down but not yet irreversibly committed to the T_H2 pathway[4, 49].

In summary, the ancestral *Ifng* locus, like the T_H2 cytokine locus, consists of three cytokine genes and a housekeeping gene whose expression must be critically controlled for proper immune responses and the prevention of autoimmunity. In the T_H2 locus, the regulation of *Il4*, *Il5* and *Il13* relies on the critical function of enhancers, silencers and a locus control region. However, the exact elements necessary for proper IFN-γ expression have not been known. We used high-resolution epigenetic mapping of the *Ifng* locus in naive, T_H1 and T_H2 cells to identify a set of enhancers and boundary elements whose patterns of accessibility coincide with potential roles in the initiation and maintenance of *Ifng* transcription in naive and T_H1 $CD4^+$ cells or the silencing of *Ifng* in T_H2 cells. The deletion of these elements *in vivo* and the identification of transcription factors binding to them and the mechanisms by which they act will help to understand more fully how these elements regulate *Ifng*.

METHODS

Mice

C57BL/6 mice were obtained from The Jackson Laboratory. All mice were housed in specific pathogen-free conditions and were maintained in accordance with procedures approved by the University of Washington's Institutional Animal Care Use Committee.

Purification and generation of T cell populations

EL-4 T cells were grown in RPMI supplement with 10% FBS, penicillin, streptomycin and L-glutamine. NK-92 cells were grown in 1x αMEM supplemented with sodium bicarbonate, 2 mM L-glutamine, 0.02 mg/ml gentamycin, penicillin, streptomycin, 12.5% fetal calf serum, 12.5% horse serum, 0.1 mM 2-mercaptoethanol, 100 U/mL recombinant human IL-2, 0.2 mM myoinositol and 0.02 mM folic acid. Smarta TCR transgenic $CD4^+$ T cells were isolated from

naïve mice using CD4 microbeads and the AutoMACS purification system or using the $CD4^+CD62L^+$ T cell isolation (Miltenyi) and gave similar results in ChIP experiments. Preparations obtained with CD4 microbead selection were >92% naïve $CD4^+CD44^{lo\text{-}int}$ T cells with <3% $CD4^+FoxP3^+$ cells, <0.5% $CD4^-Dx5^+$ NK cells, and <0.5% $CD4^+DX5^+$ NKT cells, and with the $CD4^+CD62L^+$ T cell isolation kit were >92% naïve CD4+$CD44^{lo\text{-}int}$ T cells with <0.5% $CD4^+FoxP3^+$ cells, $CD4^-DX5^+$NK cells, and NKT cells. To generate effector CD4 T cells *in vitro*, $CD4^+CD44^{lo}$ Smarta T cells were purified on a FACSAria (BD), then 0.5 x 10^6 cells were cultured in IMDM supplemented with 10% FBS, penicillin, streptomycin, 50 μM 2-mercaptoethanol and 100U/mL IL-2 (Chiron) in the presence of 2.0 x 10^6 $CD4^-CD8^-NK1.1^-CD44^{lo}$ APCs and cognate GP-61 peptide (30 μg/ml, United Biochemical Research, Inc). T_H1 culture conditions included 5 ng/mL rIL-12 (R&D Biosystems) and 10 μg/mL anti-IL-4 (NCI); T_H2 culture conditions included 50 ng/mL rIL-4 (R&D Biosystems), 50 μg/mL anti-IL-12 and 50 μg/mL anti-IFN-γ (BioSource). Cells were expanded every 2 – 3 days in IMDM with cytokines as described above; neutralizing antibodies were added only during plating and the first expansion. Cells harvested for analysis at days 7 – 8 were >99% $CD4^{high}$ and <0.5% expressed NK1.1 or MHC class II. Effector $CD4^+$ T cells were generated *in vivo* by adoptive transfer of splenocytes containing 1 x 10^5 Smarta $Thy1.1^+$ T cells into C57BL/6 mice followed 24 h later by intraperitoneal infection with 2 x 10^5 PFU LCMV-Armstrong. After 7 – 8 days, effector cells were enriched by negative-selection using biotin-labeled antibodies to B220 and NK1.1 (BD/Pharmingen), pan-murine MHC Class II (clone M5/114) and streptavidin beads (Dynal), then $CD4^+Thy1.1^+$ CD4 Smarta effectors were purified on a FACSAria to >95% purity.

Chromatin Immunoprecipitation

This was done and results were quantified as described[33] using rabbit anti-histone H3 (Abcam), anti-H3K4(me2) (Upstate Biotechnologies), anti-H3K27(me3) (Abcam) and normal rabbit immunoglobulin G as a non-specific control (Sigma). Each primer set was optimized and quantified by real-time PCR by comparison to a 5-log standard dilution of genomic DNA. After amplification, a melt curve profile was generated for each reaction to verify specificity of each primer set (primers, Supplementary Table 2 online). Samples with a difference of less than 2.0 in mean C(t) value between the specific and nonspecific IPs were considered to be not enriched. Specific IP values are reported as $([DNA_{\text{specific IP}}]-[DNA_{\text{rIgG}}])/[DNA_{10\%\text{ input}}]*100$.

Dnase HS Mapping

Chromatin profiling was performed and quantified as described[18]. Nuclei from ≥2 x 10^7 cells were isolated, left untreated or treated with DNase I, and genomic DNA was purified. A tiling path of 250 ± 25 bp amplicons were designed to span a 124 kb region surrounding *Ifng* on mouse chromosome 10. Q-PCR reactions were performed using template from untreated or DNase I-treated nuclei. After amplification, a melt curve profile was generated to verify specificity of each primer set. For each amplicon, the DNase I sensitivity score was calculated as the ratio of product obtained from DNase I-treated DNA with the product obtained from untreated DNA. The standard deviation about the mean DNase I sensitivity scores for all the amplicons in a given cell type was then determined. The DNase I sensitivity score of each amplicon was then divided by the standard deviation to give a normalized score. The amount of product was reduced in the DNase I -treated sample for DNase I sensitive regions and the normalized score thus became positive for sensitive amplicons. Normalized values were then plotted with respect to the genomic coordinates as SD above the baseline and displayed in the UCSC genome browser. Primers for sequences at HS sites are listed in Supplementary Table 1. A complete primer list is found in Supplementary Table 3.

CpG methylation

CpG methylation in the *Ifng* and *Il4* loci was quantified by sequencing of genomic DNA after bisulfite modification, PCR amplification and cloning as described[50]. Primers are listed in Supplementary Table 4.

Enhancer Assays

DNA for each element was generated with the Expand High Fidelity PCR System (Roche; primers, Supplementary Methods online) and RP-23 353-P23 bacterial artificial chromosome (Children's Hospital of Oakland Research Institute) containing the C57BL/6 *Ifng* locus as template. *Ifng*CNS-6 and *Ifng*CNS+18–20 have previously been described[7]. Products were verified by sequencing and were inserted upstream of the 9 kb *Ifng* genomic clone in pBSII (EL-4 enhancer assays) or the *Ifng* promoter-driven (−624 bp) pGL3 vector using the *MluI* and *XhoI* sites (NK and primary T cell enhancer assays). The resulting constructs were transfected into EL-4 cells along with a T-bet-pcDNA3 or empty pcDNA3 plasmid, and a control *Actb* promotor Renilla luciferase plasmid as escribed[23]. EL-4 cells were allowed to recover for 1 h at 37°C, then left untreated or stimulated with 1.5 μM ionomycin and 25 ng/mL phorbol 12-myristate 13-acetate (PMA) for 24 h before supernatants were harvested for measurement of IFN-γby ELISA and cell lysates were prepared for measurement of Renilla luciferase activity (Promega). For primary T cell transfections, $CD44^{lo\text{-}int}$ $CD4^+$ and $CD8^+$ T cells were purified from C57BL/6 mice on a FACSAria,, or using the $CD4^+CD62L^+$ T cell isolation kit for T_H0 cells, then 1.0 x 10^6 cells were stimulated in a 24-well plate precoated with anti-CD3 (5 μg/ml, FHCRC) and anti-CD28 (10 μg/ml, BD) under T_H1 or T_H2 conditions (as described above but without APCs or peptide). T_H0 and CD8 culture conditions were similar, with the exception that cultures were supplemented with IL-2 but no other cytokines or anti-cytokine antibodies. On day 7 – 8, cells were harvested and nucleofected using the Amaxa Nucleofection kit for mouse primary T cells according to manufacturer's protocol, with the following modifications. Briefly, ~5 x 10^6 $CD8^+$ or T_H2 cells per transfection were washed and cultured at 37°C in complete medium lacking IL-2 for 5 h prior to transfection and then moved to ice for 1 h. T_H0 and T_H1 cells were not washed out of IL-2, but were placed on ice for 20 min prior to transfection. Cells were resuspended at 5 x 10^6 cells/100 μl in complete nucleofection solution and mixed with 20 μg of the indicated pGL3 firefly luciferase plasmid plus 5 μg of TK-Renilla luciferase plasmid. Following transfection, cells were allowed to recover for 4 h at 37°C, then were divided equally among wells for stimulation with murine rIL-12 (5 ng/mL, R&D Systems) plus murine rIL-18 (5 ng/mL, R&D Systems), with plate-bound anti-CD3 (5 μg/mL) and anti-CD28 (10 μg/mL), or with both. Cells were stimulated for 6 h before cell lysates were prepared for measurement of dual luciferase activity (Promega). NK-92 cells were nucleofected using the Amaxa kit V per the manufacturer protocol with the following modifications: 6 x 10^6 cells were transfected with 2.5 μg TK-Renilla luciferase and 25 μg firefly luciferase plasmids. Following transfection, cells were allowed to recover for 2 h at 37°C, then were divided equally among wells for stimulation with human rIL-12 (10 ng/ml) plus murine rIL-18 (50 ng/ml), with 25 ng/ml PMA plus 1.5 μM ionomycin, or with both for 4 h, and then were harvested for measurement of luciferase activity. Primers used for cloning elements into pGL3 are listed in supplementary methods.

Boundary Element Assays

Constructs were generated and verified as described for enhancer assays using primers listed in Supplementary Methods. For insulator assays, elements were inserted upstream of the TCRδ enhancer, whereas for enhancer-blocking assays elements were inserted between the TCRδ enhancer and promoter. The resulting plasmids were linearized prior to transfection. EL-4 cells were transfected in triplicate with 10 μg of construct DNA. Cells were allowed to recover for 15 min, then diluted to 1.0 x 10^6/ml in RPMI containing 10% FBS, streptomycin

and penicillin for 48 h. Transformants were selected by plating 0.5 x 10^6 cells in medium containing 1 mg/ml active G418 (Gibco) and 0.33% agar for ~4 weeks. Colonies ≥4 mm were enumerated; total colony counts gave similar results but were not reported because of the difficulty resolving closely spaced small colonies from satellite colonies. Transfections with control plasmids (1.6 kb MINE or enhancerless) or plasmids containing CNS elements were compared to the β-Neo parent plasmid. Significance was determined using a two-tailed, unpaired Student's *t*-test using Prism 4.0 software.

Supplementary Material

Refer to Web version on PubMed Central for supplementary material.

Acknowledgements

We acknowledge C. Surh (Scripps Research Institute) and M. Bevan (University of Washington) for Thy1.1$^+$ Smarta TCR transgenic mice, T. Krumm (University of Washington) and M. Krangel (Duke University) for the E_δ-P_δ-βNeo-scs' and Pδ-BNeo-scs' constructs, and M. Kaja for LCMV-Armstrong. We thank K. Arispe and M. Weaver for technical assistance, S. Taylor for an earlier computational analysis of the *Ifng* locus, E. Eichler and M. Orr for helpful comments. This work was supported by NIH grants AI071272 and HD18184 and a grant from the March of Dimes. JRS was supported by pre-doctoral training grants from the NIH (CA009537) and Cancer Research Institute.

References

1. Ho IC, Glimcher LH. Transcription: tantalizing times for T cells. Cell 2002;109(Suppl):S109–20. [PubMed: 11983157]
2. Murphy KM, Reiner SL. The lineage decisions of helper T cells. Nat Rev Immunol 2002;2:933–44. [PubMed: 12461566]
3. Ansel KM, Lee DU, Rao A. An epigenetic view of helper T cell differentiation. Nat Immunol 2003;4:616–23. [PubMed: 12830136]
4. Szabo SJ, Sullivan BM, Peng SL, Glimcher LH. Molecular mechanisms regulating Th1 immune responses. Annu Rev Immunol 2003;21:713–58. [PubMed: 12500979]
5. Hwang ES, Szabo SJ, Schwartzberg PL, Glimcher LH. T helper cell fate specified by kinase-mediated interaction of T-bet with GATA-3. Science 2005;307:430–3. [PubMed: 15662016]
6. Usui T, et al. T-bet regulates Th1 responses through essential effects on GATA-3 function rather than on IFNG gene acetylation and transcription. J Exp Med 2006;203:755–66. [PubMed: 16520391]
7. Mullen AC, et al. Role of T-bet in commitment of TH1 cells before IL-12-dependent selection. Science 2001;292:1907–10. [PubMed: 11397944]
8. Afkarian M, et al. T-bet is a STAT1-induced regulator of IL-12R expression in naive CD4+ T cells. Nat Immunol 2002;3:549–57. [PubMed: 12006974]
9. Mullen AC, et al. Hlx is induced by and genetically interacts with T-bet to promote heritable T(H)1 gene induction. Nat Immunol 2002;3:652–8. [PubMed: 12055627]
10. Lee GR, Kim ST, Spilianakis CG, Fields PE, Flavell RA. T helper cell differentiation: regulation by cis elements and epigenetics. Immunity 2006;24:369–79. [PubMed: 16618596]
11. Young HA, et al. Expression of human IFN-gamma genomic DNA in transgenic mice. J Immunol 1989;143:2389–94. [PubMed: 2506285]
12. Zhu H, et al. Unexpected characteristics of the IFN-gamma reporters in nontransformed T cells. J Immunol 2001;167:855–65. [PubMed: 11441092]
13. Soutto M, Zhou W, Aune TM. Cutting edge: distal regulatory elements are required to achieve selective expression of IFN-gamma in Th1/Tc1 effector cells. J Immunol 2002;169:6664–7. [PubMed: 12471094]
14. Gaszner M, Felsenfeld G. Insulators: exploiting transcriptional and epigenetic mechanisms. Nat Rev Genet 2006;7:703–13. [PubMed: 16909129]
15. Valenzuela L, Kamakaka RT. Chromatin insulators (*). Annu Rev Genet 2006;40:107–38. [PubMed: 16953792]

16. West AG, Fraser P. Remote control of gene transcription. Hum Mol Genet 2005;14(Spec No 1):R101–11. [PubMed: 15809261]
17. Nardone J, Lee DU, Ansel KM, Rao A. Bioinformatics for the 'bench biologist': how to find regulatory regions in genomic DNA. Nat Immunol 2004;5:768–74. [PubMed: 15282556]
18. Dorschner MO, et al. High-throughput localization of functional elements by quantitative chromatin profiling. Nat Methods 2004;1:219–25. [PubMed: 15782197]
19. Igawa D, Sakai M, Savan R. An unexpected discovery of two interferon gamma-like genes along with interleukin (IL)-22 and -26 from teleost: IL-22 and -26 genes have been described for the first time outside mammals. Mol Immunol 2006;43:999–1009. [PubMed: 16005068]
20. Dumoutier L, Van Roost E, Ameye G, Michaux L, Renauld JC. IL-TIF/IL-22: genomic organization and mapping of the human and mouse genes. Genes Immun 2000;1:488–94. [PubMed: 11197690]
21. Vigneau S, Rohrlich PS, Brahic M, Bureau JF. Tmevpg1, a candidate gene for the control of Theiler's virus persistence, could be implicated in the regulation of gamma interferon. J Virol 2003;77:5632–8. [PubMed: 12719555]
22. Lee DU, Avni O, Chen L, Rao A. A distal enhancer in the interferon-gamma (IFN-gamma) locus revealed by genome sequence comparison. J Biol Chem 2004;279:4802–10. [PubMed: 14607827]
23. Shnyreva M, et al. Evolutionarily conserved sequence elements that positively regulate IFN-gamma expression in T cells. Proc Natl Acad Sci U S A 2004;101:12622–7. [PubMed: 15304658]
24. Bernstein BE, et al. Genomic maps and comparative analysis of histone modifications in human and mouse. Cell 2005;120:169–81. [PubMed: 15680324]
25. Agarwal S, Rao A. Modulation of chromatin structure regulates cytokine gene expression during T cell differentiation. Immunity 1998;9:765–75. [PubMed: 9881967]
26. Schneider R, et al. Histone H3 lysine 4 methylation patterns in higher eukaryotic genes. Nat Cell Biol 2004;6:73–7. [PubMed: 14661024]
27. Cao R, et al. Role of histone H3 lysine 27 methylation in Polycomb-group silencing. Science 2002;298:1039–43. [PubMed: 12351676]
28. Bracken AP, Dietrich N, Pasini D, Hansen KH, Helin K. Genome-wide mapping of Polycomb target genes unravels their roles in cell fate transitions. Genes Dev 2006;20:1123–36. [PubMed: 16618801]
29. Lee CK, Shibata Y, Rao B, Strahl BD, Lieb JD. Evidence for nucleosome depletion at active regulatory regions genome-wide. Nat Genet 2004;36:900–5. [PubMed: 15247917]
30. Chen X, Wang J, Woltring D, Gerondakis S, Shannon MF. Histone dynamics on the interleukin-2 gene in response to T-cell activation. Mol Cell Biol 2005;25:3209–19. [PubMed: 15798206]
31. Simon JA, Tamkun JW. Programming off and on states in chromatin: mechanisms of Polycomb and trithorax group complexes. Curr Opin Genet Dev 2002;12:210–8. [PubMed: 11893495]
32. Lee DU, Agarwal S, Rao A. Th2 lineage commitment and efficient IL-4 production involves extended demethylation of the IL-4 gene. Immunity 2002;16:649–60. [PubMed: 12049717]
33. Makar KW, et al. Active recruitment of DNA methyltransferases regulates interleukin 4 in thymocytes and T cells. Nat Immunol 2003;4:1183–90. [PubMed: 14595437]
34. Zhong XP, Krangel MS. An enhancer-blocking element between alpha and delta gene segments within the human T cell receptor alpha/delta locus. Proc Natl Acad Sci U S A 1997;94:5219–24. [PubMed: 9144218]
35. Gombert WM, et al. The c-myc insulator element and matrix attachment regions define the c-myc chromosomal domain. Mol Cell Biol 2003;23:9338–48. [PubMed: 14645543]
36. Grogan JL, Locksley RM. T helper cell differentiation: on again, off again. Curr Opin Immunol 2002;14:366–72. [PubMed: 11973136]
37. Avni O, et al. T(H) cell differentiation is accompanied by dynamic changes in histone acetylation of cytokine genes. Nat Immunol 2002;3:643–51. [PubMed: 12055628]
38. Fields PE, Kim ST, Flavell RA. Cutting edge: changes in histone acetylation at the IL-4 and IFN-gamma loci accompany Th1/Th2 differentiation. J Immunol 2002;169:647–50. [PubMed: 12097365]
39. Spilianakis CG, Lalioti MD, Town T, Lee GR, Flavell RA. Interchromosomal associations between alternatively expressed loci. Nature 2005;435:637–45. [PubMed: 15880101]
40. Vigneau S, et al. Homology between a 173-kb region from mouse chromosome 10, telomeric to the Ifng locus, and human chromosome 12q15. Genomics 2001;78:206–13. [PubMed: 11735227]

41. Bernstein BE, et al. A bivalent chromatin structure marks key developmental genes in embryonic stem cells. Cell 2006;125:315–26. [PubMed: 16630819]

42. Ansel KM, Djuretic I, Tanasa B, Rao A. Regulation of Th2 differentiation and Il4 locus accessibility. Annu Rev Immunol 2006;24:607–56. [PubMed: 16551261]

43. Hatton RD, et al. A distal conserved sequence element controls Ifng gene expression by T cells and NK cells. Immunity 2006;25:717–29. [PubMed: 17070076]

44. Chang S, Aune TM. Histone hyperacetylated domains across the Ifng gene region in natural killer cells and T cells. Proc Natl Acad Sci U S A 2005;102:17095–100. [PubMed: 16286661]

45. Biemont C, Vieira C. Genetics: junk DNA as an evolutionary force. Nature 2006;443:521–4. [PubMed: 17024082]

46. Xie MH, et al. Interleukin (IL)-22, a novel human cytokine that signals through the interferon receptor-related proteins CRF2-4 and IL-22R. J Biol Chem 2000;275:31335–9. [PubMed: 10875937]

47. Liang SC, et al. Interleukin (IL)-22 and IL-17 are coexpressed by Th17 cells and cooperatively enhance expression of antimicrobial peptides. J Exp Med 2006;203:2271–9. [PubMed: 16982811]

48. Koyanagi M, et al. EZH2 and histone 3 trimethyl lysine 27 associated with Il4 and Il13 gene silencing in Th1 cells. J Biol Chem 2005;280:31470–7. [PubMed: 16009709]

49. Messi M, et al. Memory and flexibility of cytokine gene expression as separable properties of human T(H)1 and T(H)2 lymphocytes. Nat Immunol 2003;4:78–86. [PubMed: 12447360]

50. Fitzpatrick DR, et al. Distinct methylation of the interferon gamma (IFN-gamma) and interleukin 3 (IL-3) genes in newly activated primary CD8+ T lymphocytes: regional IFN-gamma promoter demethylation and mRNA expression are heritable in CD44(high)CD8+ T cells. J Exp Med 1998;188:103–17. [PubMed: 9653088]

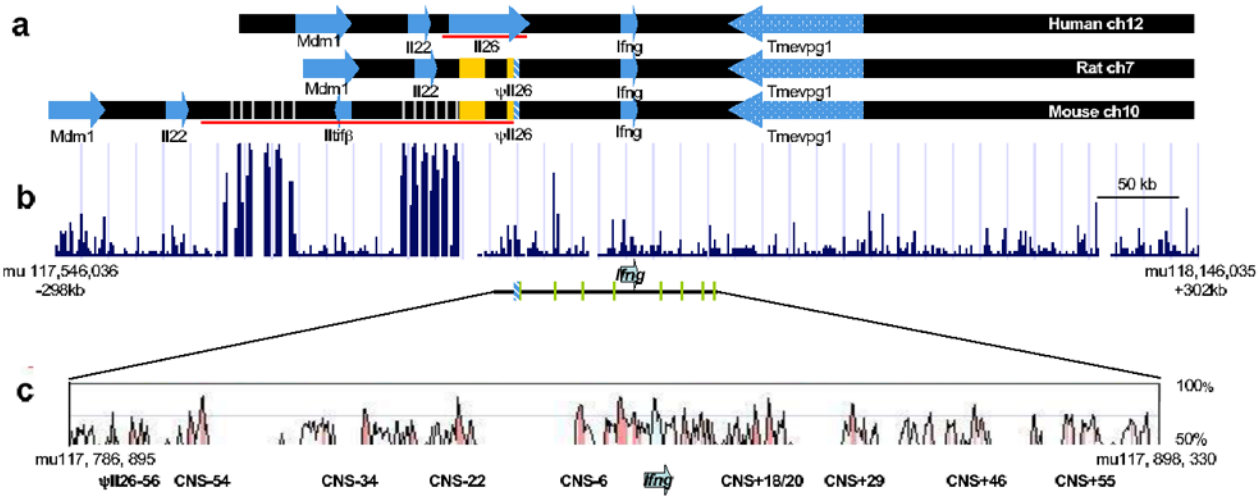

Figure 1. Evolutionary conservation within the *Ifng* locus

Alignment of 600 kb flanking the *Ifng* gene on mouse chromosome 10 with sytenic regions of rat chromosome 7 and human chromosome 12 shown (**a**) in cartoon form or (**b**) as peaks of sequence conservation using the UCSC genome browser (http://genome.ucsc.edu/cgi-bin/hgGateway). (**a**) Genes are denoted by blue arrows, indicating the direction of transcription. The stippled arrow denotes *Tmevpg1*, an antisense, non-coding transcript. Red horizontal lines below the human and mouse chromosomes indicate the location of a complex segmental duplication in the mouse genome (mm8, C57BL/6), shown in greater detail in Supplementary Fig. 1. The blue hatched bar denoted as *ΨIl26* represents sequences homologous to exon 5 of the human *IL26* gene; orange bars indicate LINE and LTR-LINE-LTR insertions described in the text. (**b**) The inset at the bottom indicates the location of the ~120 kb region surrounding *Ifng* shown in greater detail in (**c**), which displays conserved exons in turquoise and conserved non-coding sequences (CNSs) with ≥ 70% identify over ≥100 bp in red. Positions of CNSs relative to the start of murine *Ifng* are denoted below, and murine genome coordinates are shown at either end.

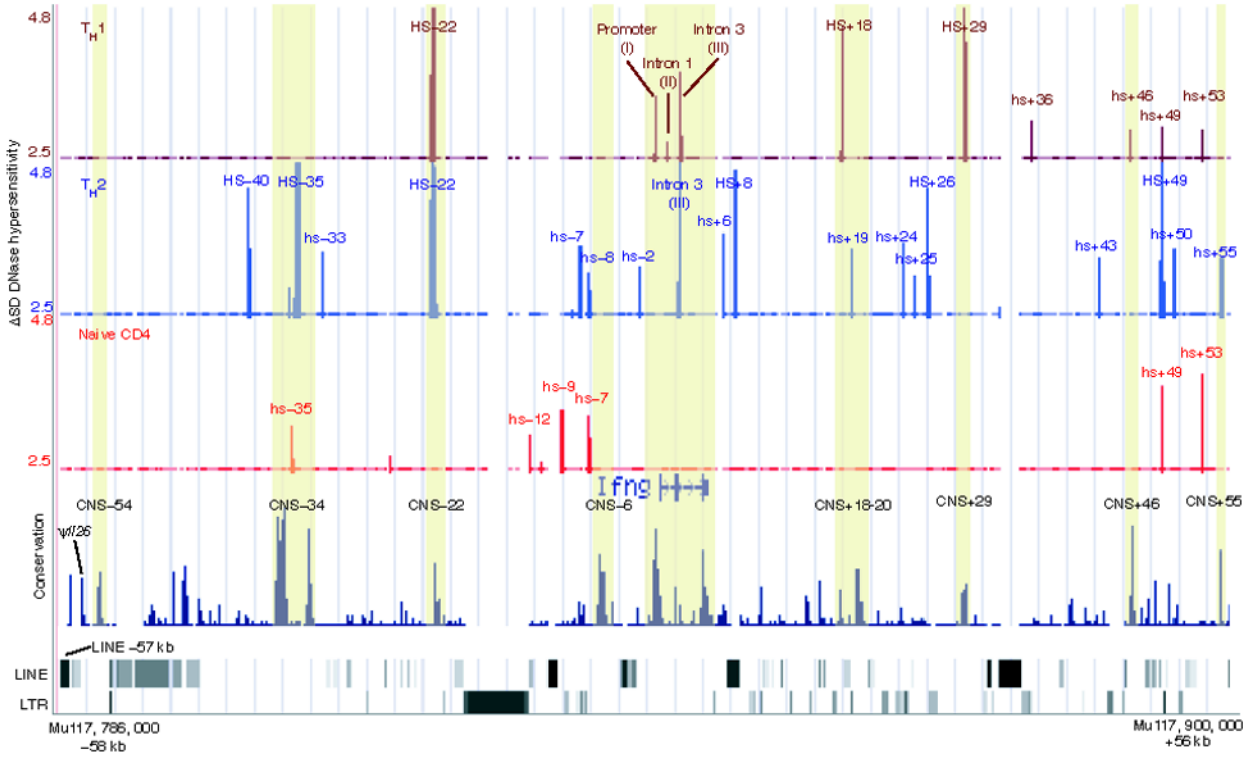

Figure 2. DNase HS profiling reveals lineage-specific changes in DNase hypersensitivity

Q-PCR was used to locate DNase HS sites in naïve, T_H1 and T_H2 cells. Genomic conservation and DNase HS sites are shown using the UCSC browser (http://genome.ucsc.edu/index.html?org=Mouse). Genome coordinates are indicated on the sides, conservation and LINE and LTR elements are shown along the bottom and the location of the CNSs are highlighted in yellow. Vertical peaks denote regions in which sensitivity to DNase digestion was ≥2.5 SD than the baseline, and peak heights represent the degree of hypersensitivity as numbers of SD. DNase HS sites are labeled based on their location relative to *Ifng*, except for sites I, II and III which are as named by Agarwal & Rao[25]. Strong HS sites (DNase I sensitivity >4SD greater than the baseline are denoted HS; weak HS sites (DNase I sensitivity >2.5 SD but < 4SD) are denoted hs. DNase profiling was done in two or more independent experiments for each cell subset, and composite results are shown.

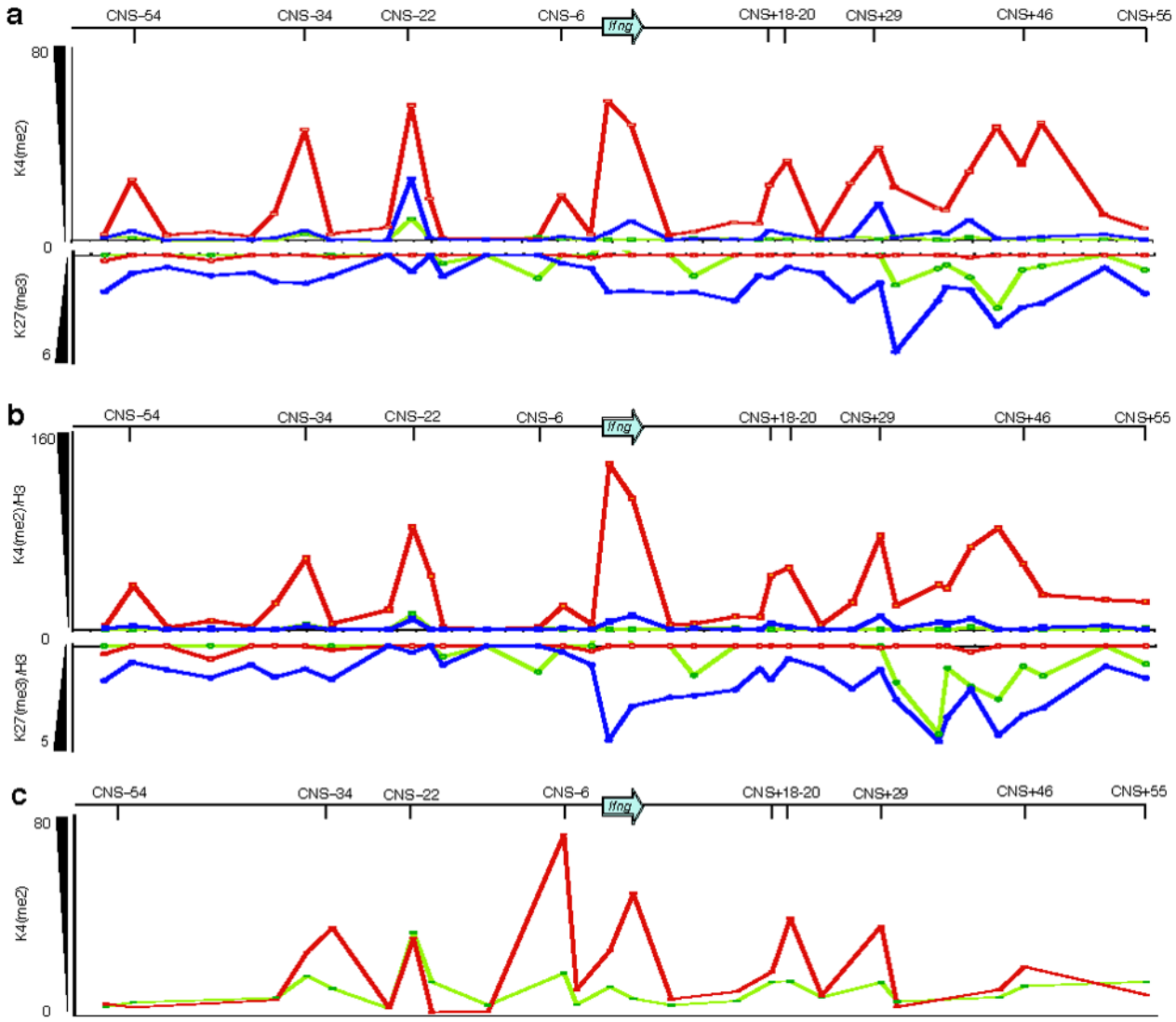

Figure 3. T_H1 cells are marked by K4(me2), whereas naive and T_H2 cells are characterized by enrichment of K27(me3)

(**a**) ChIP was used to detect enrichment of the permissive K4(me2) modification, which appears as upward-pointing peaks (top), or enrichment of the repressive K27(me3) mark, which appears as downward-pointing peaks (bottom), in naïve CD4 (light green) and *in vitro* generated T_H1 (dark red) and T_H2 cells (blue). (**b**) Enrichment of K4(me2) and K27(me3) was normalized to total histone H3 to account for possible differences in nucleosome density or structure between cell types. (**c**) ChIP for K4(me2) in naïve CD4 and T_H1 effectors generated *in vivo* following adoptive transfer into congenic mice and infection with LCMV-Armstrong. Enrichment values are arbitrary units as defined in the methods. Data are representative of three independent experiments for (**a**) and (**b**) and two independent experiments for (**c**).

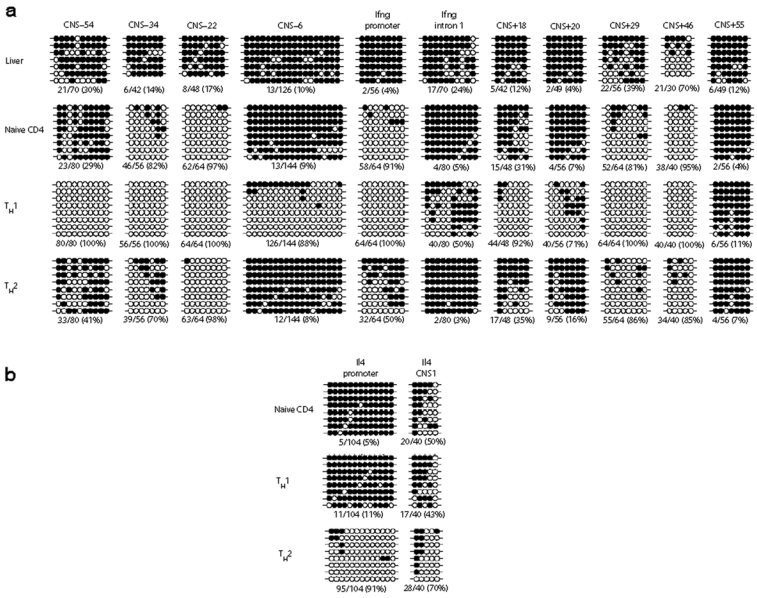

Figure 4. CD4$^+$ T cell subset-specific CpG methylation at the *Ifng* locus

Methylation of CpGs in the *Ifng* (**a**) or the *Il4–Il13* locus (**b**). CNS regions analyzed by bisulfite treatment and sequencing of cloned alleles (individual rows) are denoted at the top. Closed circles represent ^{me}CpG, open circles represent CpG. Numbers and percentage of unmethylated CpG are below each region. CpG methylation patterns from purified hepatocytes are shown as an IFN-γ non-expressing cell control. Data represent 2–4 independent experiments. For IfngCNS+55, CpG methylation was evaluated in its most distal portion centered at +59kb.

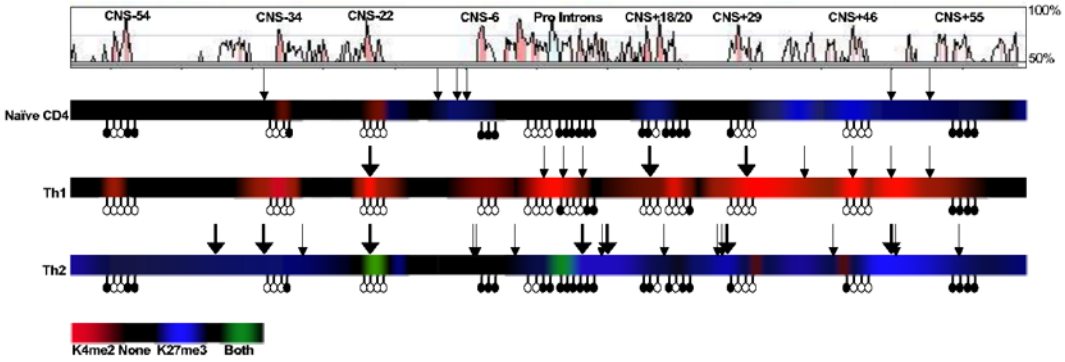

Figure 5. Epigenetic profile of naive, T_H1 and T_H2 $CD4^+$ T cells

Composite pattern of DNase HS sites (shown as downward arrows), K4(me2)/H3 (red) and K27(me3)/H3 (blue) shown as a heatmap, and methylated or unmethylated CpGs shown as filled or open lollipops, respectively, with conservation shown above in VISTA format.

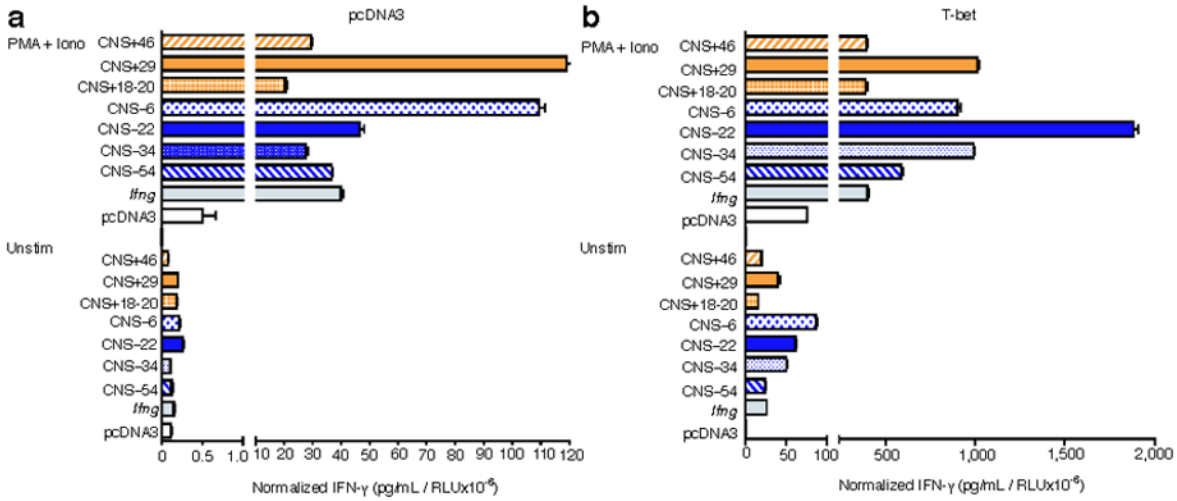

Figure 6. *Ifng*CNS–6 and *Ifng*CNS+29 enhance IFN-γ production in the absence of T-bet, whereas *Ifng*CNS–22 and IfngCNS–34 are T-bet-dependent enhancers

EL-4 cells were co-transfected with a plasmid containing the 9 kb *Ifng* gene (−3.4 to +5.6 kb) alone or also containing the indicated CNS region, and either pcDNA3 (**a**) or pcDNA3 driving expression of T-bet (**b**) plus a β-actin *Renilla* luciferase transfection control plasmid. Cells were either not stimulated (unstim) or were stimulated with PMA and ionomycin for 24 h. IFN-γwas assessed by ELISA and normalized to luciferase activity (RLU). Results are mean ± SD of duplicate samples from one representative experiment of 4 or more independent experiments.

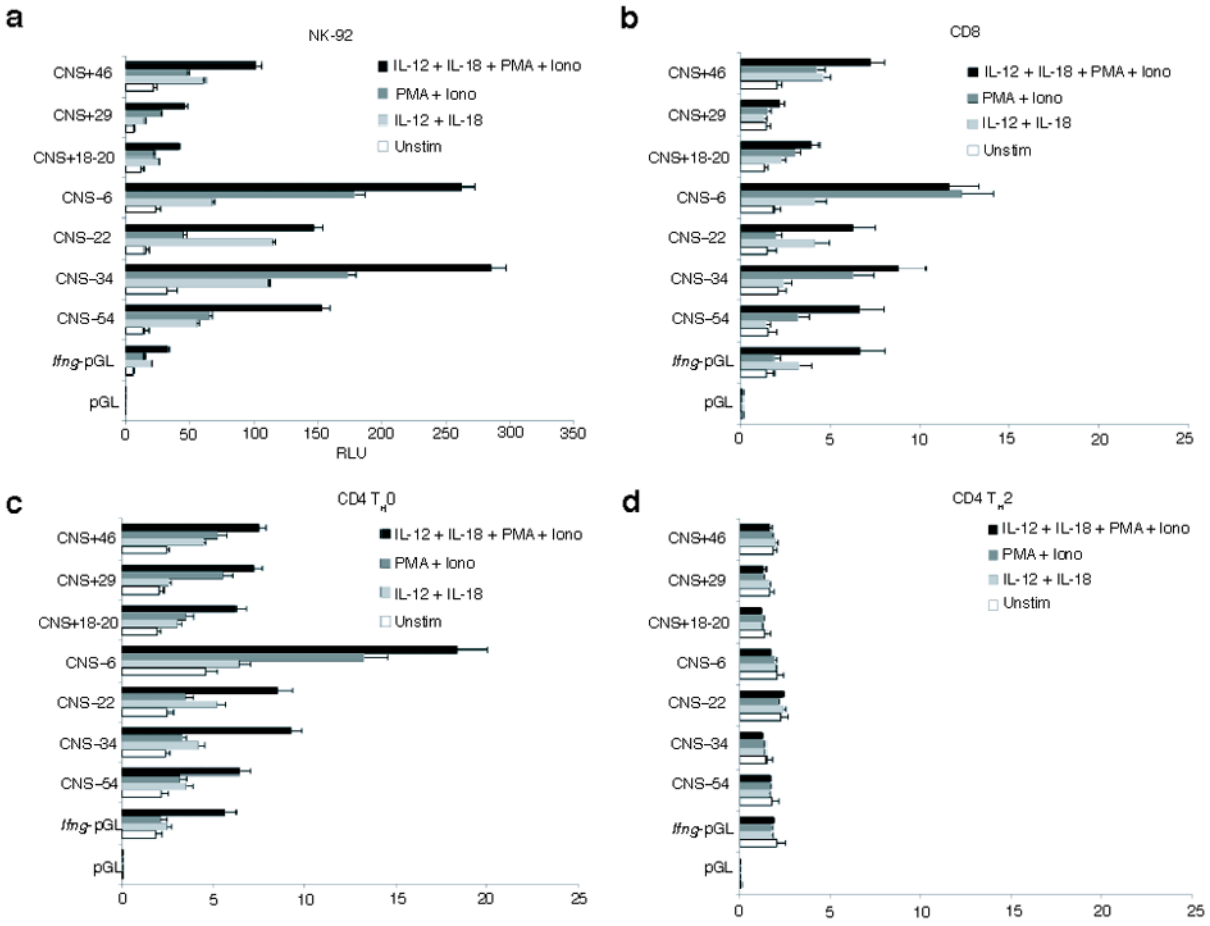

Figure 7. *Ifng* CNS elements enhance *Ifng* expression in NK cells and primary T cells

Luciferase reporter constructs containing the *Ifng* promoter and the indicated *Ifng*CNSs were transfected into NK-92 cells (**a**) or primary CD8 (**b**), T_H0 (c), or T_H2 (**d**) T cells and expression was assessed by dual luciferase assay in cells that were not stimulated or were stimulated with IL-12 plus IL-18, PMA plus ionomycin (NK-92 cells) or anti-CD3 and anti-CD28 (T cells), or the combination of these stimuli. Normalized luciferase units are mean ± SD of duplicate samples from one representative experiment of 2–5 individual experiments; results with T_H1 and T_H0 cells were similar, and a representative T_H0 experiment is shown.

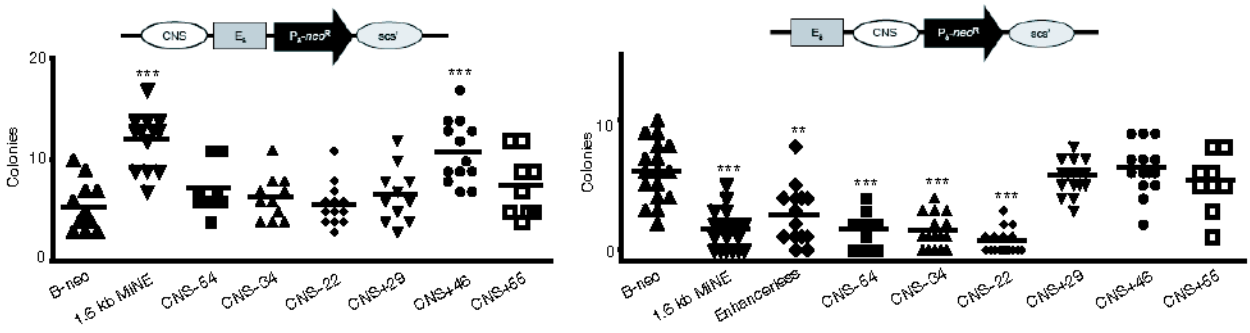

Figure 8. Boundary element function of CNSs

EL-4 cells were transfected with constructs containing the neomycin-resistance gene under the control of the TCRδpromoter and enhancer and observed for colony formation in the presence of G418 (Neo). In assays for insulator activity, CNS regions were cloned upstream of the enhancer (**a**); in assays for enhancer-blocking activity, CNS regions were cloned between the enhancer and promoter (**b**). Data are a compilation of at least three experiments, each with triplicate transfections. The bar depicts means. ***, $P \leq 0.0001$; **, $P = 0.0002$ for comparison to the β-neo control.